Journal of Medicinal Chemistry

ARTICLE

pubs.acs.org/jmc

Identification of Inhibitors that Block Vaccinia Virus Infection by Targeting the DNA Synthesis Processivity Factor D4

Manunya Nuth,[†] Lijuan Huang,[†] Yih Ling Saw,[†] Norbert Schormann,[‡] Debasish Chattopadhyay,[‡] and Robert P. Ricciardi[*,†,§]

[†]Department of Microbiology, School of Dental Medicine, University of Pennsylvania, Philadelphia, Pennsylvania 19104, United States

[‡]Department of Medicine and Center for Biophysical Sciences and Engineering, University of Alabama at Birmingham, Birmingham, Alabama 35294, United States

[§]Abramson Cancer Center, School of Medicine, University of Pennsylvania, Philadelphia, Pennsylvania 19104, United States

Supporting Information

ABSTRACT:

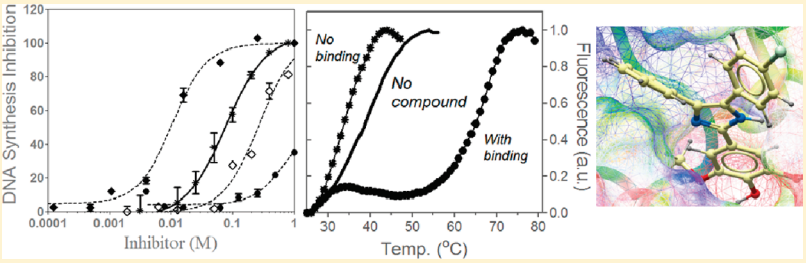

Smallpox was globally eradicated 30 years ago by vaccination. The recent threat of bioterrorism demands the development of improved vaccines and novel therapeutics to effectively preclude a reemergence of smallpox. One new therapeutic target is the vaccinia poxvirus processivity complex, comprising D4 and A20 proteins that enable the viral E9 DNA polymerase to synthesize extended strands. Five compounds identified from an AlphaScreen assay designed to disrupt A20:D4 binding were shown to be effective in: (i) blocking vaccinia processive DNA synthesis in vitro, (ii) preventing cellular infection with minimal cytotoxicity, and (iii) binding to D4, as evidenced by ThermoFluor. The EC_{50} values for inhibition of viral infectivity ranged from 9.6 to 23 μM with corresponding selectivity indices (cytotoxicity CC_{50}/viral infectivity EC_{50}) of 3.9 to 17.8. The five compounds are thus potential therapeutics capable of halting smallpox DNA synthesis and infectivity through disruptive action against a component of the vaccinia processivity complex.

INTRODUCTION

Smallpox was globally eradicated by vaccination in 1981, ending centuries of mortality numbering in the hundreds of millions. However, surreptitious stocks of variola virus, the causative agent of smallpox, pose a threat to the reemergence of this disease.[1] This concern is exacerbated by the fact that the vast portion of today's population is unvaccinated and that there is a significant number of individuals for whom the vaccine is contraindicated, e.g., those with compromised immune systems. The development of antiviral drugs that target different stages of the poxvirus life cycle is intended to provide: (i) prophylactic protection, (ii) mitigation of the disease after early onset, and (iii) prolonged time as to develop immunity following vaccination of the naïve population. Because of its extremely high sequence homology to variola virus, vaccinia virus (the vaccine agent) is the ideal laboratory strain to discover smallpox therapeutics.

Processivity factors are a new class of therapeutic targets that offer a high degree of specificity in that they interact only with their cognate DNA polymerases (Pols). Essentially, all DNA Pols fail to synthesize extended chains in the absence of associated processivity factors (PFs), often referred to as sliding clamps. The catalytic efficiency of each Pol is dependent on being tethered to the DNA template by its cognate PF, enabling the Pol to incorporate nucleotides continuously without dissociating from the template. In general, there are two classes of PFs. The first class includes the well-studied ring-shaped sliding clamps, characterized by β-subunit of *E. coli*,[2] and PCNA (proliferating cell nuclear antigen) of eukaryotic cells.[3] These ring-shaped sliding clamps completely encircle the template by using ATP-dependent clamp loaders to assemble the monomeric PF subunits around the DNA.[4] The second class of PFs does not fully encircle the DNA and hence do not require clamp loaders or ATP to associate with DNA. This includes the intensively studied herpesvirus PFs of HSV-1, EBV, and CMV,[5−8] as well as those of HHV-6 and KSHV that we discovered.[9−12] The salient feature of vaccinia and other poxviruses is that they replicate entirely within

Received: December 6, 2010
Published: March 25, 2011

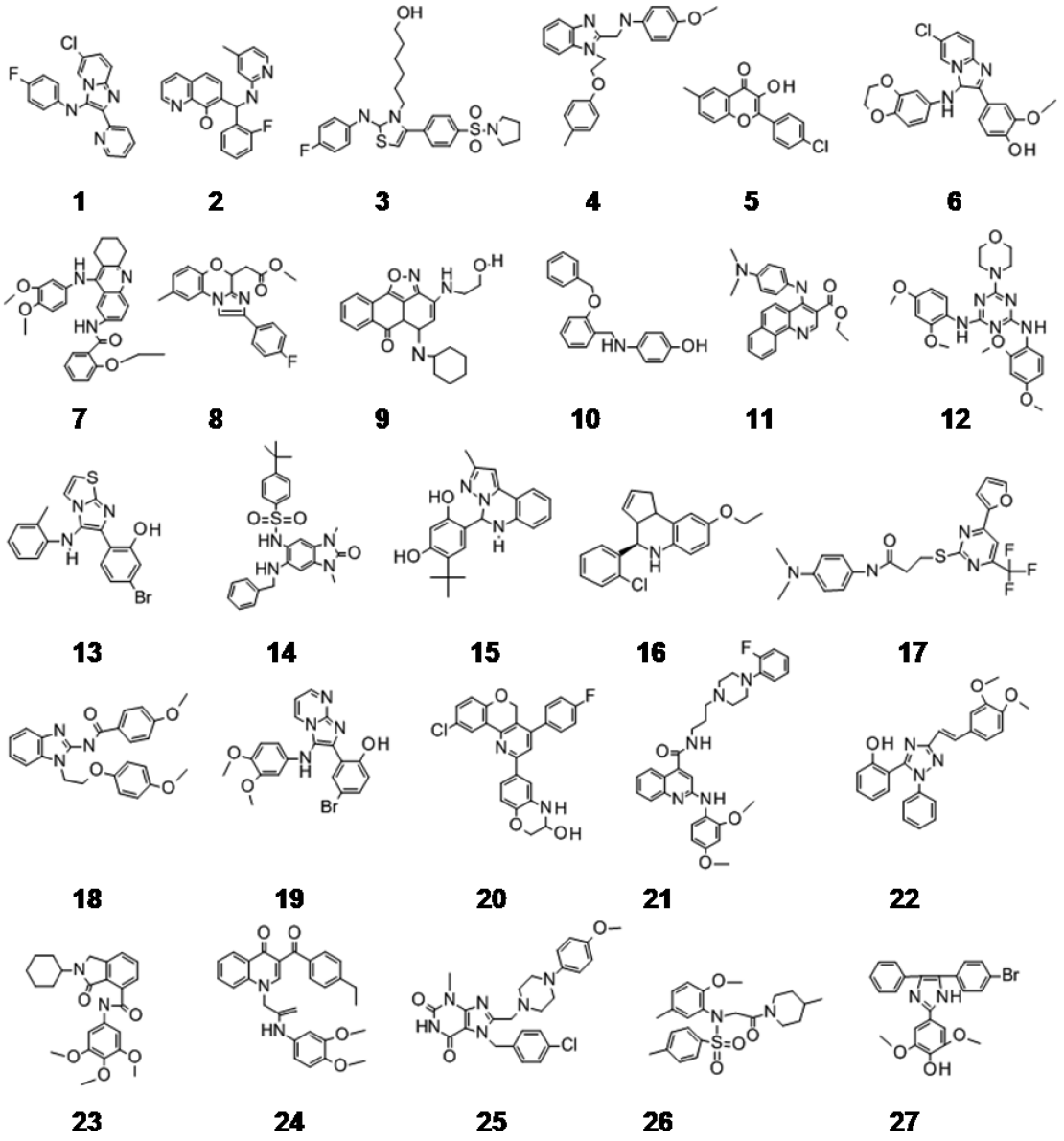

Figure 1. Hit compounds from HTS. Structures of the indentified hits represent unique chemical scaffolds.

the cytoplasm of the infected cell.[13] The 192 kb vaccinia virus genome has telomeric termini with hairpin turnarounds that link both strands.[14] Initiation of DNA synthesis occurs near the telomeres by the introduction of a nick that creates a 3′-hydroxyl primer-end from which viral E9 polymerase initiates DNA synthesis.[15] The elongated strand results in a tail-to-tail dimer that resolves to monomeric genomes.[13] All of the components for vaccinia DNA synthesis are virally encoded and include: E9 DNA polymerase,[16−18] A20 processivity factor,[19−21] D4 uracil DNA glycosylase,[22−25] D5R nucleic acid independent nucleoside triphosphatase,[26,27] and HR5,[13,28−30] along with its kinase, B1R.[31,32]

Vaccinia processive DNA synthesis in vitro is accomplished by the PF complex comprising three virally encoded proteins: E9 polymerase,[33,34] A20,[21] and D4.[35,46] Consistent with the dependence of PFs for continuous DNA synthesis, E9 Pol incorporates 10 nucleotides alone, but thousands of nucleotides in the presence of both A20 and D4.[35,46]

Although the mechanistic roles of A20 and D4 in processivity have yet to be defined, A20 could serve as a "bridge" that links E9 and D4 based on the observation that A20 interacts with both D4 and E9, whereas D4 does not interact with E9.[21,35] In addition to performing an essential role in processivity, D4 also contains a uracil DNA glycosylase (UDG) activity that can function in DNA base repair.[25,36] The dual functions of D4 appear to be mutually exclusive, as DNA synthesis is not affected by the loss of UDG activity.[37] Thus, its requirement as a processivity factor serves to explain why propagation of vaccinia is dependent on D4.[24]

D4, in particular, is an attractive drug target due to its requirement for vaccinia viability[24] as well as the availability of the protein structure.[38] In this study, we analyzed low-molecular-weight synthetic compounds that had been identified from a primary high throughput screen (AlphaScreen) that examined the disruption of the interaction of the D4 protein to the N-terminal polypeptide of A20 (Chattopadhyay et al., manuscript in preparation). In this study, 27 compounds that structurally represent

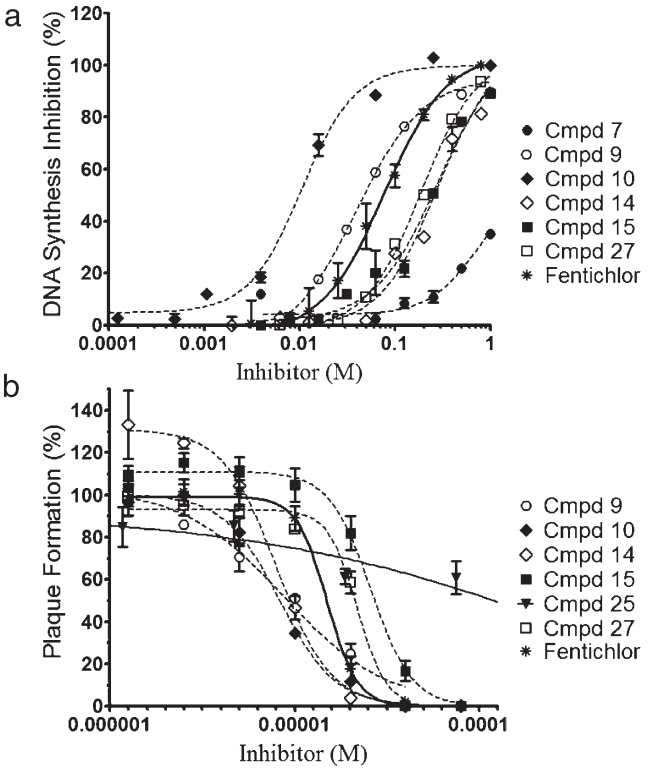

Figure 2. Functional validation of hits. (A) Inhibition VACV processive DNA synthesis. Processive DNA synthesis was conducted using the rapid plate assay in which extended strand synthesis is quantified by the incorporation of DIG-dUTP. The percent inhibition was calculated relative to the uninhibited negative control (DMSO) and the completely inhibited positive control (EDTA). (B) Inhibition of VACV infection. BSC-1 cells were cultured to confluence and infected with vaccinia virus to achieve ~80 PFU/well on a 48-well well plate. DMSO was maintained at 1%, and the representative dose−response curves are shown for both assays. Experiments were performed in triplicates and repeated at least twice. For comparison, Fentichlor, a known processive DNA synthesis inhibitor,[41] was employed.

the hits from the primary screen were evaluated for their abilities to functionally disable processive DNA synthesis in vitro and block viral infection in cells. Five compounds were identified to be effective at reducing viral plaques with low cytotoxicity. Significantly, the compounds were further shown to target D4 through the use of a thermal stability assay. Thus, these D4 inhibitors are the first reported to target a specific component of the vaccinia processivity complex and have the potential to serve as therapeutics capable of preventing the spread of smallpox.

RESULTS AND DISCUSSION

Selection of Hits from a D4:A20 AlphaSreen. A high throughput screening (HTS) by AlphaScreen designed to select for compounds that disrupt the interaction between D4 and the N-terminal 100 amino acids of A20 was utilized and is described elsewhere (Chattopadhyay et al., manuscript in preparation). Hits were identified from 28000 compounds that demonstrated appreciable inhibition of the interaction when added at 33 μM. In addition to their abilities to disrupt the D4:A20 interaction by at least 85%, the compounds were further selected based on known low toxicity and reactivity according to the ICCB-Longwood database (Chattopadhyay et al., manuscript in preparation). For this study, 27 of the 88 hit compounds, representing nonredundant chemical scaffolds with CLogP values of approximately 5 or less, were selected for further validation. The structures of these 27 hit compounds are shown in Figure 1.

Functional Validation: Rapid Plate Assay. To test whether the hit compounds were capable of blocking processive DNA synthesis, we employed the functional rapid plate assay.[39−41] Briefly, the assay consists of a biotinylated primer-DNA template (100 bp) attached to a streptavidin-coated 96-well plate, whereby processivity is assessed by the ability of E9 to incorporate nucleotides for DNA strand extension in the presence of A20 and D4. Representative dose−response curves used to extract IC_{50} values are shown in Figure 2A, with Fentichlor, which was previously shown to effectively block processive DNA synthesis,[41] serving as comparison (IC_{50} = 38.5 μM). Fifteen of the compounds (**1**, **3**, **4**, **6**, **8**, **12**, **13**, **16**, **19**, **20**, **21**, **22**, **23**, **24**, and **25**) displayed IC_{50} values ≥200 μM and were thus considered to be either incapable or inefficient in functionally blocking processive DNA synthesis. In contrast, 10 compounds (**2**, **5**, **7**, **11**, **14**, **15**, **17**, **18**, **26**, and **27**) effectively inhibited DNA synthesis with IC_{50} values between 50 and 200 μM. Only two of the compounds, **9** and **10**, were very effective at blocking processive DNA synthesis with IC_{50} values of 34.1 and 5.1 μM, respectively. The IC_{50} values for the 27 compounds are summarized in Table 1.

Vaccinia Virus Plaque Reduction and Cytotoxicity. Next, the 27 compounds were tested in a plaque reduction assay to determine their effectiveness in preventing viral infection. To obtain plaques that are readily distinct, a low multiplicity of infection of BSC-1cell monolayers was used to generate about 80 plaques in each well of a 48-well plate. Dose−response curves used to extract EC_{50} values are depicted in Figure 2B. Consistently, Fentichlor is effective against viral infection (EC_{50} = 18.7 μM). Inhibitory results are summarized in Table 1. Despite negligible inhibition of DNA synthesis, compounds **1**, **2**, and **3** displayed high potency (EC_{50} = 2.9−3.8 μM), while compounds **5**, **8**, **12**, **22**, **23**, **24**, **25** and **26** exhibited no detectable inhibitory activities (≥200 μM). The rest of the compounds showed significant (<10 μM) to modest inhibitory activity (13−75 μM). Importantly, compounds **9** and **10**, which displayed effective DNA synthesis inhibition (IC_{50} = 34.1 and 5.1 μM, respectively), were also effective against viral infection (EC_{50} = 8.1 and 7.1 μM, respectively) while exhibiting relatively low cytotoxicity (CC_{50} = 127.3 and 175.4 μM, respectively). In all, 14 compounds exhibited CC_{50} values ranging from 23.3 to 175.4 μM, while the other 13 compounds showed negligible cytotoxicity (CC_{50} > 200 μM). Results are summarized in Table 1.

Identification of Hit Compounds that Target Vaccinia Virus D4. With the identification of promising candidates that appeared to halt viral infection via interference to the processivity complex, we sought to investigate D4 as a potential target. This was further emphasized in the design of the AlphaScreen HTS, which specifically looked at disruption to A20 and D4 interaction. As such, we examined thermal protein denaturation as a means for extracting binding information. The ThermoFluor method is based on the energetic coupling between ligand and protein unfolding.[42] Thus, the change of the unfolding transition temperature (ΔT_m) reflects the binding affinity between the unliganded protein and the protein−ligand complex, whereby the melting temperature (T_m) is determined from the protein unfolding midpoint. Indeed, ThermoFluor has been successfully employed for compound screening.[43−45] Moreover, there is

Table 1. Summary of Antiviral and Functional Activities of HTS Compound Hits[a]

compound (source)	CLogP	DNA synthesis IC_{50} (μM)	plaque reduction EC_{50} (μM)	cytotoxicity[b] CC_{50} (μM)	selectivity index[c]
1 (C177−0169)	5.0	>200	3.8	>200	53
2 (7706−0074)	4.3	157.3	2.9	>200	69
3 (8009−1110)	5.0	>200	3.2	>200	63
4 (C147−0148)	5.3	>200	5.5	121.1	22
5 (7170−3687)	4.8	194.7	nd	>200	nd
6 (C273−0442)	4.6	>200	10.8	>200	18
7 (C619−0600)	5.2	105.8	>200	73.7	11
8 (8539−0704)	4.9	>200	>200	84.1	0.4
9 (C620−0278)	4.5	34.1	8.4	127.3	15
10 (6408−0250)	4.0	5.1	7.1	175.4	25
11 (5174−4519)	6.0	139.1	nd	>200	nd
12 (5594−3013)	0.6	>200	nd	169.6	nd
13 (C239−0873)	6.9	>200	>200	141.9	9
14 (C301−6073)	4.1	132.1	18.8	>200	>10
15 (7210−1961)	2.9	137.6	21.5	92.8	4
16 (5408−0925)	6.4	221	22.4	>200	9
17 (7213−0271)	4.3	140	>200	57.2	4
18 (7292−0026)	4.9	168.6	47.9	23.2	0.5
19 (C325−0463)	4.2	200	67.6	>200	3
20 (8539−0659)	5.6	>200	74.6	>200	3
21 (C387−0301)	4.0	>200	25.8	>200	8
22 (5169−1136)	5.7	>200	>200	106.8	0.5
23 (C447−0998)	2.6	>200	>200	>200	nd
24 (C647−0648)	5.5	>200	>200	52.9	0.3
25 (C692−0362)	2.5	>200	>200	92.8	0.4
26 (3786−0771)	3.3	175.3	nd	>200	nd
27 (5218−0975)	5.3	91.2	16.7	57.2	3
Fentichlor	nd	38.5	18.7	nd	nd

[a] Half-maximal values (EC_{50}, IC_{50} and CC_{50}) were determined from triplicate measurements and repeated at least twice. Apparent values beyond 200 μM (designated >200 μM) were deemed unreliable due to difficulty in compound solubitity or otherwise not determined (nd). Log *P* values (CLogP) were calculated by the ACD/Laboratories software (Advanced Chemisty Development, Inc.). [b] Determined by measuring LDH released into the medium. [c] Determined by CC_{50}/EC_{50}.

good agreement of ThermoFluor to more conventional methods such as isothermal titration calorimetry and enzymatic assays.[43]

Here, we used the ThermoFluor method to determine which of the hit compounds is capable of interacting with D4 (Table 2). A positive ΔT_m reflects inhibitor binding, manifested as stabilization of the protein upon denaturation. In contrast, a negative ΔT_m indicates that the protein is destabilized as a result of adventitious binding by inhibitor, and a lack of change (within experimental error) suggests no ligand−protein interaction. Selected thermograms are depicted in Figure 3B for a nonbinder (compound **19**, ΔT_m = −0.1 °C) and a nonspecific binder (compound **23**, ΔT_m = −4.9 °C). Indeed, modest plaque reduction (EC_{50} = 67.6 μM) and poor DNA synthesis activities (IC_{50} = 200 μM) were observed for **19**, thus suggesting the likelihood of target(s) other than D4 (e.g., A20) responsible for the plaque inhibitory effect. In contrast, the negative ΔT_m value for **23** is consistent with nonspecific binding to D4, which may account for the lack of activities for both assays. Of particular note are compounds **1**, **2**, and **3**. Despite exhibiting potency against viral infection, negative ΔT_m values were observed, thus ruling out the targeting of D4 as a likely mode of action. Most significantly, as shown in Figure 3, positive ΔT_m values were observed for compounds **9** (ΔT_m = 13.1 °C), **10** (ΔT_m = 14.9 °C), **14** (ΔT_m = 10.0 °C), **15** (ΔT_m = 4.9 °C), and **27** (ΔT_m = 4.6 °C), which are strongly indicative of binding to D4. Strikingly, all five compounds were effective at reducing viral infection (EC_{50} = 9.6, 9.8, 18.8, 23.3, and 22.4 μM, respectively) and inhibiting processive DNA synthesis (IC_{50} = 34.1, 5.1, 132.1, 137.6, and 91.2 μM, respectively). Values of all five compounds (Table 1) were comparable to that of Fentichlor, a known inhibitor of processive DNA synthesis.[41]

Molecular Docking. In an effort to understand the potential binding mechanism, the five lead compounds were docked to the VACV D4 utilizing ICM-Pro. Compound **10** showed preferred docking within proximity of the UDG catalytic pocket, which is outlined by K126, K160, and R187 (Figure 3C), amino acids recently shown to be essential for D4 processivity, but not UDG activity.[46] Compounds **14** showed a similar preference as **10** (Supporting Information SI4). In contrast, compounds **9** and **15**, in addition to docking near the UDG catalytic site, showed an additional preference within proximity of the loop region between helix 5 and β-sheet 4, comprising residues K54, Q55, and P56 (Supporting Information SI3 and SI4). A third docking site at loop regions comprising residues R61, T149, K150, and H151 was observed for compound **27**, in addition to the UDG catalytic site and the loop region between helix 5 and β-sheet 4 (Supporting Information SI4).

CONCLUSIONS

Therapeutic compounds are needed to prevent a smallpox attack arising from a surreptitious release of variola virus. The D4 and A20 vaccinia virus proteins are nearly identical to those of variola and have the potential to serve as excellent antiviral targets because they are both essential for processive DNA synthesis. Discovering and developing therapeutics that target D4 is all the more attractive because its crystal structure has been determined.[38] A previous HTS campaign of 28000 synthetic compounds identified disruptors of D4 and A20 interaction (Chattopadhyay et al., manuscript in preparation). In this study, 27 of the hit compounds with unique scaffolds were further investigated in a series of secondary assays. We identified five compounds that showed the ability to interact with D4, in addition to exhibiting favorable inhibitory activities against vaccinia virus infection and processive DNA synthesis. Molecular docking revealed all five lead compounds to show a preference for regions nearby the UDG catalytic site comprising the amino acids K126, K160, and R187, which have recently been shown to be important in processivity.[46] An additional binding pocket was observed for compounds **9** and **15**, while a third binding pocket was identified for compound **27**. Because amino acids K126, K160, and R187 are important for processivity, we speculate that perturbation to these residues either by direct binding of compound or by protein conformational change induced by distal compound binding will result in disruption of processivity. Future studies will confirm if this site on D4 is a preferred binding site for these compounds and serve as the basis for lead optimization.

Table 2. Protein Denaturation Summary for Interactions of Vaccinia Virus D4 with Small Molecule Compounds[a]

hit	T_m (°C)	ΔT_m (°C)	hit	T_m (°C)	ΔT_m (°C)
DMSO mock	38.4 ± 1.6	0.0	**14**	48.4 ± 6.0	10.0
1	34.7 ± 1.5	−3.7	**15**	44.3 ± 3.7	4.9
2	36.4 ± 0.4	−2.0	**16**	35.2 ± 2.0	−5.0
3	35.1 ± 0.7	−3.3	**17**	35.1 ± 1.8	−1.7
4	35.2 ± 1.0	−3.2	**18**	34.3 ± 0.7	−4.1
5	36.4 ± 1.3	−2.0	**19**	38.3 ± 1.3	−0.1
6	36.9 ± 1.0	−1.5	**20**	34.9 ± 1.3	−3.5
7	36.3 ± 0.9	−2.1	**21**	34.8 ± 1.5	−3.6
8	32.2 ± 0.3	−6.6	**22**	34.7 ± 0.4	−3.7
9	51.4 ± 9.1	13.1	**23**	33.2 ± 0.3	−4.9
10	53.3 ± 1.5	14.9	**24**	35.4 ± 0.4	−3.2
11	36.3 ± 0.5	−1.5	**25**	35.9 ± 0.8	−2.5
12	35.0 ± 0.4	−3.4	**26**	33.6 ± 2.0	−4.8
13	36.5 ± 1.2	−1.9	**27**	43.0 ± 3.0	4.6

[a] Experiments were performed using 4 μM D4 in the presence or absence of 50 μM compounds in 25 mM Tris, pH 7.2, 0.15 M NaCl, 5 mM $ZnCl_2$, and 1% DMSO. T_m values are shown ± SD from at least three independent experiments (n = 3−5), with thermal shift (ΔT_m) values obtained by the subtraction of the untreated DMSO mock.

The identified compounds are novel in that they are the first described to target D4. Of the five, compounds **9** (10-(cyclohexylamino)-12-[(2-hydroxyethyl)amino]-15-oxa-14-azatetracyclohexadeca-1(16),2,4,6,9,11,13-heptaen-8-one) and **10** (4-({[2-(benzyloxy)phenyl]methyl}amino)phenol) appeared to be the most potent, followed by compounds **14** (*N*-[6-(benzylamino)-1,3-dimethyl-2-oxo-2,3-dihydro-1*H*-1,3-benzodiazol-5-yl]-4-*tert*-butylbenzene-1-sulfonamide), **15** (4-*tert*-butyl-6-{2-methyl-5*H*,6*H*-pyrazolo[1,5-*c*]quinazolin-5-yl}benzene-1,3-diol), and **27** (4-[5-(4-bromophenyl)-4-phenyl-1*H*-imidazol-2-yl]-2,6-dimethoxyphenol) (Table 3). Compound **2**, which lacked D4 binding, was shown to be effective in preventing vaccinia virus infection (SI = 69). The ability to block DNA synthesis to some extent suggests that it likely targets a component of the processivity complex other than D4. Future studies will shed light onto whether A20 or E9 is, in fact, a target of compound **2**. In conclusion, we have identified several compounds that effectively suppress vaccinia virus infection as a consequence of blocking processive DNA synthesis by directly targeting D4.

EXPERIMENTAL SECTION

Reagents. Reagents used were purchased from Sigma-Aldrich, unless otherwise noted, and used without further purification. Digoxigenin-11-2′-deoxyuridine-5′-triphosphate (DIG-dUTP), streptavidin-coated 96-well plates, and the DIG detection ELISA kit were purchased from Roche Applied Science (Indianapolis, IN). LDH cytotoxicity detection kit was purchased from Takara Bio Inc. (Madison, WI) and Sypro Orange from Invitrogen (Carlsbad, CA) as 5000X DMSO stock.

Cells and Viruses. African green monkey kidney epithelial cells (BSC-1) were maintained in DMEM supplemented with 5% fetal calf serum (growth medium), 10 U/mL penicillin, and 10 μg/mL streptomycin in a humidified incubator at 37 °C, 5% CO_2. Cells were not used beyond 10 passages. Vaccinia virus (WR strain) was a kind gift from Dr. Gary H. Cohen (University of Pennsylvania).

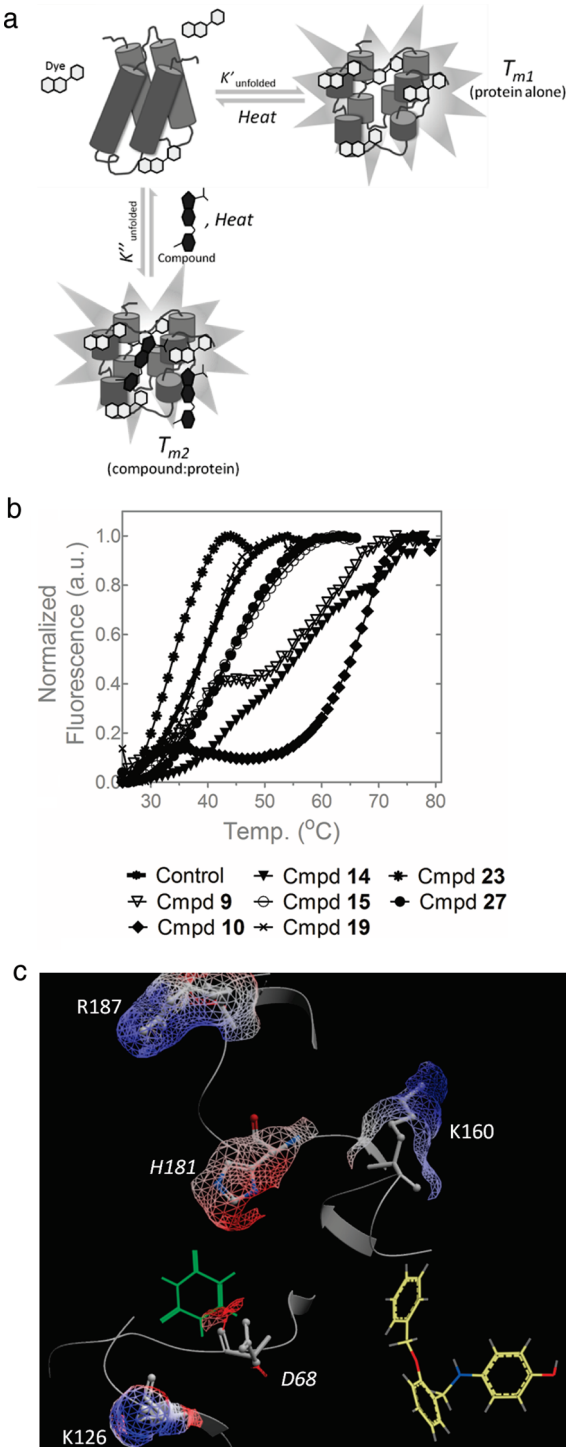

Figure 3. Assessment of compound binding by ThermoFluor. (A) As heat was applied, protein denaturation was measured spectrofluorimetrically with the hydrophobic dye, Sypro Orange. Any perturbation produced when a compound is added is reflected in the thermal shift (ΔT_m), which is the difference in the unliganded (T_{m1}) and liganded complex (T_{m2}). (B) The thermograms of various compounds are shown, with the 1% DMSO mock indicated by the solid trace. (C) Structural representation of uracil (green) and compound **10** (yellow) docked to the VACV D4. The catalytic acid/base (H181/D68) of the UDG pocket and the amino acids shown to be important in processivity are presented. Both uracil and compound **10** conformations represent high-ranked poses as scored by ICM-Pro.

dx.doi.org/10.1021/jm101554k |*J. Med. Chem.* 2011, 54, 3260–3267

Table 3. Property Summary of Compound Leads

hit	molecular weight	solubility[a] (μg/mL)	solubility (μM)
9	377.436	1.4	3.6
10	305.370	1.1	3.5
14	478.606	0.9	1.9
15	349.426	19.1	54.7
27	451.313	1.4	3.2

[a] Solubility of compound in PBS was determined by measuring the chemiluminescence of total nitrogen contents (www.aniliza.com).

Chemical Hit Compounds. A high throughput AlphaScreen of 28000 compounds is described elsewhere (Chattopadhyay et al., manuscript in preparation). Samples for the current study were chosen from the ChemDiv 6 library and were selected for chemical scaffold uniqueness and, preferably, CLogP $\leq$ 5. A few compound exceptions, however, were selected with CLogP values >5 in order to completely represent unique scaffolds within the ChemDiv 6 library. The 27 compounds were purchased from ChemDiv and were verified by the vendor to be greater than 90% pure ($\geq$95% typical) by liquid chromatography−mass spectrometry (LC-MS) on a Shimadzu HPLC and API 150EX mass spectrometer and by ^{1}H nuclear magnetic resonance (NMR) using a Bruker DPX-400 instrument.

Preparation of Vaccinia Virus D4 Protein. D4 was cloned from VACV WR strain into pET15 harboring an N-terminal His_6 construct as previously described.[38] Briefly, the D4 construct was expressed in *E. coli* Rosetta(DE3)pLysS cells and induced with IPTG overnight at 18 °C in LB, followed by column purification with Ni-NTA and gel filtration. His_6 tag removal was accomplished with thrombin, yielding a native protein of approximately 25 kDa.

Processivity Assessment by Rapid Plate Assay. Inhibitors that disrupted processive DNA synthesis were identified by the rapid plate assay as previously described.[39−41] Briefly, the ELISA-based method was performed in streptavidin-coated 96-well plates. To achieve processivity, the biotinylated template (5′-biotinAGCACTA TTGA-CATTACAGAGT CGCCTTGGCTCTCTG GCTGTTCGTTGC GGGCTCCGCGTG CGTTGGCTTCGGTC GTCCCGTCAGCGG TCATTCATTGGC-3′) permitted the incorporation of DIG-dUTP largely at the distal end of the synthesized DNA product. The corresponding primer used to anneal to the template was 5′-GCC AAT GAA TGA CCG CTG AC-3′. Plate preparation was accomplished by coating 5 μM of the annealed primer-template and thoroughly washing with PBS. A typical DNA synthesis reaction was performed in 50 μL volume consisting of 1 μL each of in vitro translated proteins (A20, D4, and E9) in 100 mM $(NH_4)_2SO_4$, 20 mM Tris-HCl pH 7.4, 3 mM $MgCl_2$, 0.1 mM EDTA, 0.5 mM DTT, 2% glycerol, 40 μg/mL BSA, 5 μM dNTPs, and 1 μM DIG-dUTP. One microliter of test compounds of varying concentrations dissolved in DMSO was added individually to each well. One microliter of DMSO or EDTA was used as corresponding positive or negative control, respectively. The plates were then incubated at 37 °C for 30 min and colorimetrically developed using the DIG detection ELISA kit. IC_{50} values were determined from measurements at 405 nm on a microplate reader. Each compound was tested in triplicate of 2-fold serial dilutions of three or more independent experiments.

Viral Plaque Reduction Assay. Confluent BSC-1 monolayers in 48-well plates were obtained by seeding 2×10^4 cells/well in 300 μL of growth medium and cultured overnight. Cells were infected by adsorbing virus for 1 h in a humidified incubator at 80 PFU/well in 100 μL of growth medium, followed by overnight treatment with inhibitors done in triplicate of each concentration in a final volume of 300 μL of growth medium and 1% DMSO. Cells were subsequently fixed with 300 μL of 5% formaldehyde in PBS for 6 h at room temperature, followed by 30 min staining with 5% crystal violet, washed twice with distilled H_2O, air-dried overnight, and counted.

Cytotoxicity. Cytotoxicity was assessed by the measurement of lactate dehydrogenase (LDH) in the medium according to the manufacturer's recommendation. Briefly, BSC-1 cells were seeded in a 96-well optical plate at 1×10^4 cells/well in 100 μL of growth medium. After 24 h, the growth medium was replaced with fresh medium containing inhibitors, adjusted to 1% DMSO, and incubated for an additional 20 h. Then 100 μL of LDH reaction mixture was added into each well. The plate was incubated at room temperature in the dark for 30 min, and the absorbance at 492 nm was measured on a microplate reader. Each compound was tested using 2-fold serial dilutions performed in triplicates, and experiments were independently repeated three times. Treatment with 2% Triton X-100 served as the positive control for maximum LDH release, while 1% DMSO served as negative control.

Thermal Stability Assay. A typical experiment was performed using a 96-well thin-wall PCR plate at 20 μL total volume in 25 mM Tris-HCl, pH 7.2 consisting of 4 μM D4, 0.15 M NaCl, and 5 mM $ZnCl_2$. All inhibitors were prepared at 5 mM in DMSO and added to give 50 μM final inhibitor and 1% DMSO concentrations. Proteins were exhaustively dialyzed into Tris buffer prior to use. Sypro Orange was diluted 1:200 in Tris buffer and was immediately added to give 5× working concentration. Fluorescence intensities were monitored by a charge-coupled device camera on the Applied Biosystems 7500 Fast Real-Time PCR system (Carlsbad, CA) using the TAMRA filter (582 nm emission) from 25 to 80 °C at a scan rate of 1 °C/min. Raw intensity values were exported and fitted to a Boltzmann model,

$$F = \mathrm{Pre} + \left(\frac{(\mathrm{Post} - \mathrm{Pre})}{1 + \exp\left(\frac{T_m - T}{\mathrm{slope}}\right)} \right)$$

where F is the fluorescence intensity at temperature T, and T_m the protein unfolding transition midpoint. Pre and Post represent the respective pretransitional and posttransitional values, where slope defines the steepness of the curve. Thermal shift (ΔT_m) is the difference between the 1% DMSO mock treatment and inhibitor treatment. All experiments were repeated at least three times.

Molecular Docking. Docking of the compounds was accomplished using the ICM-Pro software (Molsoft L.L.C., La Jolla, CA, version 3.7-2a).[47] The *E. coli* UDG (PDB accession no. 2EUG) and the trigonal crystal form of VACV D4 (PDB accession no. 2OWQ)[38] served as protein receptors. Bound ligands and cofactors were removed from the proteins prior to converting into ICM objects to be used for docking. Compounds were drawn with Symyx Draw 4.0 (Accelrys, San Diego, CA) and uploaded into ICM-Pro. The integrity of the software was initially tested by docking uracil to *E. coli* UDG, and the identified poses were in good agreement with the X-ray crystallographic structure of the uracil bound to the same protein. Eight conformations were identified exhibiting rmsd values ranging from 2.92 for the highest (ICM score $E = -37.01$) to 3.68 for the lowest-ranked (ICM score $E = -28.91$) conformation (Supporting Information SI1 and SI2). Typically, an ICM score of −32 or lower is considered favorable. We then proceeded to dock the five lead compounds. Results are given in Supporting Information (SI3 and SI4).

Data Analysis. Half-maximal (EC_{50}, IC_{50}, and CC_{50}) values were obtained by nonlinear regression fitting to a variable slope, four parameter dose−response model using the Prizm software (GraphPad Software, LaJolla, CA).

■ ASSOCIATED CONTENT

Supporting Information. Docked conformations of uracil and the five lead compounds. This material is available free of charge via the Internet at http://pubs.acs.org.

AUTHOR INFORMATION

Corresponding Author

*Phone: 215-898-3905. Fax: 215-898-8385. E-mail: Ricciard@upenn.edu.

ACKNOWLEDGMENT

This work was supported by the National Institutes of Health grant 5U01-A1 082211 to R.P.R.

ABBREVIATIONS USED

HTS, high throughput screening; PF, processivity factor; UDG, uracil DNA glycosylase; VACV, vaccinia virus

REFERENCES

(1) Longini, I. M., Jr.; Halloran, M. E.; Nizam, A.; Yang, Y.; Xu, S.; Burke, D. S.; Cummings, D. A.; Epstein, J. M. Containing a large bioterrorist smallpox attack: a computer simulation approach. *Int. J. Infect. Dis.* **2007**, *11*, 98–108.

(2) Kong, X. P.; Onrust, R.; O'Donnell, M.; Kuriyan, J. Three-dimensional structure of the beta subunit of E. coli DNA polymerase III holoenzyme: a sliding DNA clamp. *Cell* **1992**, *69*, 425–437.

(3) Krishna, T. S.; Kong, X. P.; Gary, S.; Burgers, P. M.; Kuriyan, J. Crystal structure of the eukaryotic DNA polymerase processivity factor PCNA. *Cell* **1994**, *79*, 1233–1243.

(4) Ellison, V.; Stillman, B. Opening of the clamp: an intimate view of an ATP-driven biological machine. *Cell* **2001**, *106*, 655–660.

(5) Gottlieb, J.; Marcy, A. I.; Coen, D. M.; Challberg, M. D. The herpes simplex virus type 1 UL42 gene product: a subunit of DNA polymerase that functions to increase processivity. *J. Virol.* **1990**, *64*, 5976–5987.

(6) Kiehl, A.; Dorsky, D. I. Cooperation of EBV DNA polymerase and EA-D(BMRF1) in vitro and colocalization in nuclei of infected cells. *Virology* **1991**, *184*, 330–340.

(7) Tsurumi, T.; Daikoku, T.; Kurachi, R.; Nishiyama, Y. Functional interaction between Epstein−Barr virus DNA polymerase catalytic subunit and its accessory subunit in vitro. *J. Virol.* **1993**, *67*, 7648–7653.

(8) Weiland, K. L.; Oien, N. L.; Homa, F.; Wathen, M. W. Functional analysis of human cytomegalovirus polymerase accessory protein. *Virus Res.* **1994**, *34*, 191–206.

(9) Agulnick, A. D.; Thompson, J. R.; Iyengar, S.; Pearson, G.; Ablashi, D.; Ricciardi, R. P. Identification of a DNA-binding protein of human herpesvirus 6, a putative DNA polymerase stimulatory factor. *J. Gen. Virol.* **1993**, *74* (Pt 6), 1003–1009.

(10) Lin, K.; Dai, C. Y.; Ricciardi, R. P. Cloning and functional analysis of Kaposi's sarcoma-associated herpesvirus DNA polymerase and its processivity factor. *J. Virol.* **1998**, *72*, 6228–6232.

(11) Lin, K.; Ricciardi, R. P. The 41 kDa protein of human herpesvirus 6 specifically binds to viral DNA polymerase and greatly increases DNA synthesis. *Virology* **1998**, *250*, 210–219.

(12) Chen, X.; Lin, K.; Ricciardi, R. P. Human Kaposi's sarcoma herpesvirus processivity factor-8 functions as a dimer in DNA synthesis. *J. Biol. Chem.* **2004**, *279*, 28375–28386.

(13) Beaud, G. Vaccinia virus DNA replication: a short review. *Biochimie* **1995**, *77*, 774–779.

(14) Baroudy, B. M.; Venkatesan, S.; Moss, B. Structure and replication of vaccinia virus telomeres. *Cold Spring Harbor Symp. Quant. Biol.* **1983**, *47* (Pt 2), 723–729.

(15) Pogo, B. G.; O'Shea, M.; Freimuth, P. Initiation and termination of vaccinia virus DNA replication. *Virology* **1981**, *108*, 241–248.

(16) Traktman, P.; Kelvin, M.; Pacheco, S. Molecular genetic analysis of vaccinia virus DNA polymerase mutants. *J. Virol.* **1989**, *63*, 841–846.

(17) Jones, E. V.; Moss, B. Mapping of the vaccinia virus DNA polymerase gene by marker rescue and cell-free translation of selected RNA. *J. Virol.* **1984**, *49*, 72–77.

(18) Traktman, P.; Sridhar, P.; Condit, R. C.; Roberts, B. E. Transcriptional mapping of the DNA polymerase gene of vaccinia virus. *J. Virol.* **1984**, *49*, 125–131.

(19) Ishii, K.; Moss, B. Role of vaccinia virus A20R protein in DNA replication: construction and characterization of temperature-sensitive mutants. *J. Virol.* **2001**, *75*, 1656–1663.

(20) Punjabi, A.; Boyle, K.; DeMasi, J.; Grubisha, O.; Unger, B.; Khanna, M.; Traktman, P. Clustered charge-to-alanine mutagenesis of the vaccinia virus A20 gene: temperature-sensitive mutants have a DNA-minus phenotype and are defective in the production of processive DNA polymerase activity. *J. Virol.* **2001**, *75*, 12308–12318.

(21) Klemperer, N.; McDonald, W.; Boyle, K.; Unger, B.; Traktman, P. The A20R protein is a stoichiometric component of the processive form of vaccinia virus DNA polymerase. *J. Virol.* **2001**, *75*, 12298–12307.

(22) Ellison, K. S.; Peng, W.; McFadden, G. Mutations in active-site residues of the uracil-DNA glycosylase encoded by vaccinia virus are incompatible with virus viability. *J. Virol.* **1996**, *70*, 7965–7973.

(23) Millns, A. K.; Carpenter, M. S.; DeLange, A. M. The vaccinia virus-encoded uracil DNA glycosylase has an essential role in viral DNA replication. *Virology* **1994**, *198*, 504–513.

(24) Stuart, D. T.; Upton, C.; Higman, M. A.; Niles, E. G.; McFadden, G. A poxvirus-encoded uracil DNA glycosylase is essential for virus viability. *J. Virol.* **1993**, *67*, 2503–2512.

(25) Upton, C.; Stuart, D. T.; McFadden, G. Identification of a poxvirus gene encoding a uracil DNA glycosylase. *Proc. Natl. Acad. Sci. U. S.A.* **1993**, *90*, 4518–4522.

(26) Evans, E.; Traktman, P. Characterization of vaccinia virus DNA replication mutants with lesions in the D5 gene. *Chromosoma* **1992**, *102*, S72–82.

(27) Evans, E.; Klemperer, N.; Ghosh, R.; Traktman, P. The vaccinia virus D5 protein, which is required for DNA replication, is a nucleic acid-independent nucleoside triphosphatase. *J. Virol.* **1995**, *69*, 5353–5361.

(28) Beaud, G.; Beaud, R. Preferential virosomal location of under-phosphorylated H5R protein synthesized in vaccinia virus-infected cells. *J. Gen. Virol.* **1997**, *78* (Pt 12), 3297–3302.

(29) DeMasi, J.; Traktman, P. Clustered charge-to-alanine mutagenesis of the vaccinia virus H5 gene: isolation of a dominant, temperature-sensitive mutant with a profound defect in morphogenesis. *J. Virol.* **2000**, *74*, 2393–2405.

(30) Murcia-Nicolas, A.; Bolbach, G.; Blais, J. C.; Beaud, G. Identification by mass spectroscopy of three major early proteins associated with virosomes in vaccinia virus-infected cells. *Virus Res.* **1999**, *59*, 1–12.

(31) Banham, A. H.; Smith, G. L. Vaccinia virus gene B1R encodes a 34-kDa serine/threonine protein kinase that localizes in cytoplasmic factories and is packaged into virions. *Virology* **1992**, *191*, 803–812.

(32) Lin, S.; Chen, W.; Broyles, S. S. The vaccinia virus B1R gene product is a serine/threonine protein kinase. *J. Virol.* **1992**, *66*, 2717–2723.

(33) McDonald, W. F.; Traktman, P. Vaccinia virus DNA polymerase. In vitro analysis of parameters affecting processivity. *J. Biol. Chem.* **1994**, *269*, 31190–31197.

(34) McDonald, W. F.; Traktman, P. Overexpression and purification of the vaccinia virus DNA polymerase. *Protein Expr. Purif.* **1994**, *5*, 409–421.

(35) Stanitsa, E. S.; Arps, L.; Traktman, P. Vaccinia virus uracil DNA glycosylase interacts with the A20 protein to form a heterodimeric processivity factor for the viral DNA polymerase. *J. Biol. Chem.* **2006**, *281*, 3439–3451.

(36) Holzer, G. W.; Falkner, F. G. Construction of a vaccinia virus deficient in the essential DNA repair enzyme uracil DNA glycosylase by a complementing cell line. *J. Virol.* **1997**, *71*, 4997–5002.

(37) De Silva, F. S.; Moss, B. Vaccinia virus uracil DNA glycosylase has an essential role in DNA synthesis that is independent of its glycosylase activity: catalytic site mutations reduce virulence but not virus replication in cultured cells. *J. Virol.* **2003**, *77*, 159–166.

(38) Schormann, N.; Grigorian, A.; Samal, A.; Krishnan, R.; DeLucas, L.; Chattopadhyay, D. Crystal structure of vaccinia virus uracil-DNA glycosylase reveals dimeric assembly. *BMC Struct. Biol.* **2007**, *7*, 45.

(39) Ricciardi, R. P.; Lin, K.; Chen, X.; Dorjsuren, D.; Shoemaker, R.; Sei, S. Rapid screening of chemical inhibitors that block processive DNA synthesis of herpesviruses: potential application to high-throughput screening. *Methods Mol. Biol.* **2005**, *292*, 481–492.

(40) Ciustea, M.; Silverman, J. E.; Druck Shudofsky, A. M.; Ricciardi, R. P. Identification of non-nucleoside DNA synthesis inhibitors of vaccinia virus by high-throughput screening. *J. Med. Chem.* **2008**, *51*, 6563–6570.

(41) Silverman, J. E.; Ciustea, M.; Shudofsky, A. M.; Bender, F.; Shoemaker, R. H.; Ricciardi, R. P. Identification of polymerase and processivity inhibitors of vaccinia DNA synthesis using a stepwise screening approach. *Antiviral Res.* **2008**, *80*, 114–123.

(42) Pantoliano, M. W.; Petrella, E. C.; Kwasnoski, J. D.; Lobanov, V. S.; Myslik, J.; Graf, E.; Carver, T.; Asel, E.; Springer, B. A.; Lane, P.; Salemme, F. R. High-density miniaturized thermal shift assays as a general strategy for drug discovery. *J. Biomol. Screen.* **2001**, *6*, 429–440.

(43) Lo, M. C.; Aulabaugh, A.; Jin, G.; Cowling, R.; Bard, J.; Malamas, M.; Ellestad, G. Evaluation of fluorescence-based thermal shift assays for hit identification in drug discovery. *Anal. Biochem.* **2004**, *332*, 153–159.

(44) Abad, M. C.; Askari, H.; O'Neill, J.; Klinger, A. L.; Milligan, C.; Lewandowski, F.; Springer, B.; Spurlino, J.; Rentzeperis, D. Structural determination of estrogen-related receptor gamma in the presence of phenol derivative compounds. *J. Steroid Biochem. Mol. Biol.* **2008**, *108*, 44–54.

(45) Ericsson, U. B.; Hallberg, B. M.; Detitta, G. T.; Dekker, N.; Nordlund, P. Thermofluor-based high-throughput stability optimization of proteins for structural studies. *Anal. Biochem.* **2006**, *357*, 289–298.

(46) Druck Shudofsky, A. M.; Silverman, J. E. Y.; Chattopadhyay, D.; Ricciardi, R. P. Vaccinia virus D4 mutants defective in processive DNA synthesis retain binding to A20 and DNA. *J. Virol.* **2010**, *84*, 12325–12335.

(47) Abagyan, R. A.; Totrov, M. M; Kuznetsov, D. A. ICM: A New Method For Protein Modeling and Design: Applications to Docking and Structure Prediction From The Distorted Native Conformation. *J. Comput. Chem.* **1994**, *15*, 488–506.